Strahlenther Onkol (2016) 192:92–101
DOI 10.1007/s00066-015-0929-9

ORIGINAL ARTICLE

Lipiodol versus diaphragm in 4D-CBCT-guided stereotactic radiotherapy of hepatocellular carcinomas

Mark K. H. Chan · Venus Lee · C. L. Chiang · Francis A. S. Lee · Gilbert Law · N. Y. Sin · K. L. Siu · Frank C. S. Wong · Stewart Y. Tung · Hollis Luk · Oliver Blanck

Received: 1 August 2015 / Accepted: 20 November 2015 / Published online: 3 December 2015

Abstract
Purpose The purpose of this work was to investigate the potential of lipiodol as a direct tumor surrogate alternative to the diaphragm surrogate on four-dimensional cone-beam computed tomography (4D-CBCT) image guidance for stereotactic radiotherapy of hepatocellular carcinomas.
Methods A total of 29 hepatocellular carcinomas (HCC) patients treated by stereotactic radiotherapy following transarterial chemoembolization (TACE) with homogeneous or partial defective lipiodol retention were included. In all, 4–7 pretreatment 4D-CBCT scans were selected for each patient. For each scan, either lipiodol or the diaphragm was used for 4D registration. Resulting lipiodol/diaphragm motion ranges and position errors relative to the reconstructed midventilation images were analyzed to obtain the motion variations, and group mean (ΔM), systematic (Σ), and random (σ) errors of the treatment setup.
Results Of the lipiodolized tumors, 55% qualified for direct localization on the 4D-CBCT. Significant correlations of lipiodol and diaphragm positions were found in the left–right (LR), craniocaudal (CC), and anteroposterior (AP) directions. ΔM and σ obtained with lipiodol and diaphragm were similar, agreed to within 0.5 mm in the LR and AP, and 0.3 mm in the CC directions, and Σ differed by 1.4 (LR), 1.1 (CC), and 0.6 (AP) mm. Variations of diaphragm motion range >5 mm were not observed with lipiodol and in one patient with diaphragm. The margin required for the tumor prediction error using the diaphragm surrogate was 6.7 (LR), 11.7 (CC), and 4.1 (AP) mm.
Conclusion Image-guidance combining lipiodol with 4D-CBCT enabled accurate localization of HCC and thus margin reduction. A major limitation was the degraded lipiodol contrast on 4D-CBCT.

Keywords Image-guided radiotherapy · 4D cone beam CT · Stereotactic body radiotherapy · Contrast media · Planning techniques

M. K. H. Chan (✉) · V. Lee · C. L. Chiang · F. A. S. Lee · G. Law · F. C. S. Wong · S. Y. Tung · H. Luk
Department of Clinical Oncology, TuenMun Hospital, TuenMun, Hong Kong (S.A.R)
e-mail: ckh456@ha.org.hk

N. Y. Sin · K. L. Siu
Department of Diagnostic Radiology, TuenMun Hospital, TuenMun, Hong Kong (S.A.R)

O. Blanck
Department of Radiation Oncology, Saphir Radiosurgery Center, University Clinic Schleswig–Holstein, Kiel, Germany

Lipiodol versus Zwerchfell in 4D-CBCT-geführter stereotaktischer Strahlentherapie bei hepatozellulären Karzinomen

Zusammenfassung
Hintergrund Ziel dieser Studie war es, das Potential von Lipiodol als direktes Tumorsurrogat alternativ zum Zwerchfellsurrogat für die vierdimensionale Cone-beam-Computertomographie (4D-CBCT) in der stereotaktischen Strahlentherapie von hepatozellulären Karzinomen (HCC) zu analysieren.
Methoden Eingeschlossen wurden 29 HCC-Patienten, die mittels stereotaktischer Strahlentherapie nach transarterieller Chemoembolisation (TACE) mit homogener oder teilweise defekter Lipiodolspeicherung behandelt wurden. Für jeden Patienten wurden 4–7 4D-CBCT-Scans vor der Behandlung ausgewählt. Für jeden Scan wurde

eine 4-D-Registrierung unter Verwendung von Lipiodol oder Zwerchfell als Registrierungsmaske durchgeführt. Die resultierenden Lipiodol- bzw. Zwerchfellbewegungen und Positionsfehler relativ zu den rekonstruierten MidP-Bildern (MidV, midventilation images) wurden analysiert, um Veränderungen in den Bewegungen, Gruppen- (ΔM), systematische (Σ) und zufällige (σ) Fehler in der Patientenlagerung sowie notwendige Sicherheitssäume (M) beurteilen zu können.

Ergebnisse Für die direkte Lokalisierung auf den 4D-CBCT waren 55 % der Tumoren mit Lipiodol geeignet. Signifikante Korrelationen von Lipiodol- und Zwerchfellpositionen wurden in links-rechts (LR), kraniokaudalen (CC) und anteroposterioren (AP) Richtungen gefunden. Die ΔM- und σ-Fehler mit Lipiodol und Zwerchfell stimmten mit Abweichungen von 0,5 mm in LR- und AP- sowie mit 0,3 mm in CC-Richtung überein; der Σ-Fehler unterschied sich um 1,4 mm (LR), 1,1 mm (CC) und 0,6 mm (AP). Veränderungen der Zwerchfellbewegung >5 mm wurden bei keinem Patienten mit Lipiodol und bei einem Patienten mit Zwerchfell als Registrierungsmaske beobachtet. Der notwendige Sicherheitssaum, um den Tumorvorhersagefehler für das alleinige Zwerchfellsurrogat auszugleichen, betrug 6,7 mm (LR), 11,1 mm (CC) und 4,1 mm (AP).

Schlussfolgerung Bildregistrierungsprotokolle mit Lipiodol in Kombination mit 4D-CBCT ermöglichen die genaue Lokalisierung von HCC und somit die signifikante Reduktion von Sicherheitssäumen. Haupteinschränkungen dieser Technik sind bereits abgebaute Lipiodolanreicherungen auf dem 4D-CBCT.

Schlüsselwörter Bildgeführte Strahlentherapie · 4D-Cone-Beam-Computertomographie · Stereotaktische Körperbestrahlung · Kontrastmittel · Planungstechnik

Image-guidance (IG) is impeccable for hypofractionated/stereotactic body radiotherapy (SBRT) of hepatocellular carcinomas (HCC) to achieve safety margin reduction and hence minimization of radiation to normal tissues. Because the tumor contrast with surrounding tissue is often too low for direct target localization during treatment, surrogates such as implanted metal markers or diaphragm/liver contour are used, in some situations demanding considerable margin to account for the uncertainty in the correlation between the surrogate and the tumor [1].

For patients who had prior transcatheter arterial chemoembolization with lipiodol (TACE) in combined treatment therapy, the retention of intense tumor stain due to selective uptake of lipiodol by tumor cells that generally remains for several weeks [2] can serve as a natural contrast medium for direct image-guided tumor targeting [3, 4].

At our institute, the image-guidance solution is based on linac-integrated four-dimensional (4D)-CBCT, which technically is similar to the 4D-CT in the way that the CBCT images are reconstructed at different positions along the respiratory cycle [5]. It has the possibility of reconstructing CBCT images corresponding to the time-weighted average position at which we aim for tumor targeting. The advantage of targeting the tumor at its time time-weighted average position has been discussed extensively in the literature [5, 6], being able to minimize the systematic errors from tumor motion. The major application of 4D-CBCT so far has been focusing on treatments of lung tumors [7, 8], and experience in applying it to HCC are relatively limited [9, 10] notably owing to the poor tumor contrast. Case et al. [9, 10] were among the first demonstrating off-line the feasibility of 4D-CBCT-guided treatments of HCCs. However, they were unable to localize the tumor directly without prior lipiodol but relying on the diaphragm as a surrogate. Because of the lobe dependence of tumor motion in the liver [11, 12], population statistics about the inter- and intrafractional liver motion and position provided by Case et al. [9, 10] were of limited applicability in terms of formulating the safety margin.

In this study, we aimed to (1) investigate the potential of lipiodol for direct target localization on 4D-CBCT, (2) assess the uncertainties of interfractional treatment setup, interfractional tumor baseline, and motion amplitude estimated by the lipiodol and the diaphragm using 4D-CBCT, and (3) provide an assessment of the margin required for diaphragm/lipiodol-guided treatment setup.

Methods and materials

Patients and treatment

A total of 29 patients with single primary nonresectable HCC were enrolled in this retrospective analysis approved by the Institutional Review Board. Transcatheter arterial chemoembolization (TACE) was performed by supraselective cannulation of the supplying tumor artery. An emulsion was prepared by mixing lipiodol with cisplatin in a 1:1 ratio. Various amounts of the emulsion were injected slowly under fluoroscopic monitoring according to the size of the tumor and the arterial blood flow. Maximum dosage of cisplatin and lipiodol injected was 40 mg and 20 ml for each treatment session, respectively. The interval between TACE and 4D-CT simulation was 1 week, and was 3–4 weeks to radiotherapy. The prescription dose was individualized to either 4 Gy for 6–10 fractions or 6–9 Gy for 6 fractions at 77–87 % prescription isodose lines relative to the maximum dose by a risk-adaptive approach.

Immobilization, 4D-CT simulation, and treatment planning

Immobilization of the patients was achieved by a Vac-Lok cushion (MEDTEC, Orange City, IA, USA). Optimal abdominal compression was applied to all patients to achieve minimal while reproducible tumor motion. For each patient, 3 mm slice thickness 4D-CT images were acquired in helical mode on a Philips Brilliance Big Bore 16-slice CT scanner (Philips Medical Systems, Cleveland, OH, USA) and phase-sorted into ten bins of equal time share of the respiratory cycle. The TACE lipiodol was used as contrast medium in all 4D-CT scans to assist target delineation. Based on the lipiodol contrast on the 4D CT scan, the tumor trajectory and motion range was estimated for the three cardinal directions: *x, y* and *z* corresponding to the left–right (LR), craniocaudal (CC), and anteroposterior (AP) directions, respectively. Next, the time-weighted mean tumor position (MidP) and its corresponding time-percentage were calculated as described in our previous study [13], and 1 of the initial 10 4D-CT phases that was closest to this mid-ventilation (MidV) time percentage was selected for tumor delineation, treatment planning, and as the reference images for image guidance. Note that the MidV alternative of MidP ignored the fact that some tumors exhibited hystersis over their breathing trajectories. Therefore, a small systematic error would be introduced. The mean tumor vector error of MidV relative to the MidP approach has been estimated at 1.0±0.5 mm, which was within image resolution [14].

The safety margin M from the gross tumor volume (GTV) to the planning target volume (PTV) that aimed to ensure 95% minimum dose to the GTV for 90% of the population was calculated by combining the individual motion amplitude with the population motion uncertainties by $M = 2.5\Sigma + \beta\sqrt{\left(\sigma^2 + \sigma_p^2\right)} - \beta\cdot\sigma_p$, where Σ and σ are the components of systematic and random errors including tumor delineation, 4D-CT/CBCT registration, and intrafractional baseline drift, β=1.03 for 85% isodose level (IDL) and σ_p=3.2 mm for penumbra in water [7]. We assumed that tumor delineation and 4D-CT/CBCT registration each contributed to error of 1 mm. Furthermore, the statistics about intrafractional baseline drift was adapted from Case et al. [9, 10] in the lack of in-house data. SmartArc (Pinnacle^3 v.9.2, Philips Radiation Oncology Systems, Fitchburg, WI, USA) was used to create volumetric arc radiotherapy (VMAT) plans to achieve the dose constraints per our institutional HRT protocol.

CBCT image-guidance correction protocol

Pretreatment CBCT was acquired at each fraction with the 4D Symmetry protocol (XVI R4.5, Elekta Oncology Systems, Crawley, UK). Each 4D-CBCT scan acquired 1320 projection images at 5.5 frames per second over 200° in 4 minutes. The XVI software implemented a feature-based algorithm to extract the respiratory trace for sorting the projections into ten bins according to the respiratory phase, thus, removing the need of external respiratory monitoring. Each bin was then separately reconstructed to yield a three-dimensional (3D)-CBCT data set. The 4D correction protocol described by Sonke et al. [7] was followed in this study, which involved a two-stage registration procedure. After the CBCT acquisition, a bone registration was first performed by a user-defined 3D region-of-interest (ROI) placed around the vertebrae in the MidV reference CT, yielding three rotational and three translational errors. Next, a 3D ROI so-called mask expanded from the planning contour of either the GTV (lipiodol-based) or the liver (diaphragm-based) was automatically registered to each phase of a 4D-CBCT scan by local rigid registrations. This step resulted in an estimated target trajectory relative to the reference CT and a displacement of the time-weighted mean position (MidP) that was used for couch correction. During 4D registration, only translations were optimized ignoring rotations and deformations. For this reason, rotation errors were limited to <1.5° in the previous bone registration or the patient was repositioned. At this point, the registration was visually inspected, and the necessary adjustment was made by a single expert oncologist to avoid interobserver variability.

All patients were treated by the strategy described above as planning and treating the tumor at MidP, which has been shown to facilitate margin reduction compared to the use of internal target volume (ITV; [6]). Prior to each delivery, we further ensured that the motion range in each direction estimated with the lipiodol/diaphragm mask on the 4D-CBCT was no larger than that estimated on the planning 4D-CT by 3 mm, which required roughly an additional 2 mm margin for motion range of 1–10 mm [7, 15].

Quantitative assessment of the lipiodol/diaphragm position on 4D-CBCT data

Only lipiodol retention that was classified as homogeneous accumulation and partial defect [16] in both the simulation 4D-CT and treatment verification 4D-CBCT scans was considered as an acceptable surrogate for inclusion in the analysis. A total of 186 4D-CBCT scans were analyzed, with 4–7 scans per patient including the first and last scans and other 2–5 scans in between. The interfractional changes of absolute tumor position (i.e., treatment setup) were analyzed separately for IG correction protocols using the centroid positions of the lipiodol and liver contours at MidP. The interfractional change of absolute lipiodol/diaphragm position was obtained from the result of 4D registration of each scan as the difference of lipiodol/diaphragm at MidP on the 4D-CBCT compared with the lipiodol at MidV on the

planning 4D-CT. Pearson's correlation coefficient (r) was used to assess the relationship of the interfractional changes of the absolute lipiodol and diaphragm positions.

Impact of lipiodol for target localization and motion estimation

Lipiodol was hypothesized to provide the reference treatment setup in our online correction protocol. Diaphragm-guided treatment setup was used when the lipiodol had become invisible on the 4D-CBCT. The difference between the reference lipiodol-based and the diaphragm-based registration provided the tumor prediction error **e** of a diaphragm-guided treatment setup. For each patient, **e** was calculated for all scans to obtain the mean tumor prediction error $\bar{e}_{x/y/z}$ for the LR/CC/AP directions. Because the motion of liver tumors is lobe dependent, we measured the distance from the tumor to the diaphragm (D) to understand its relationship with $\bar{e}_{x/y/z}$. D was measured from the 4D-CT simulation scan as the distance from the dome of the diaphragm to the last seen GTV contour in the cranial direction. The norm of the mean tumor prediction error $\bar{e}_{x/y/z}$ $\geq$1/3/5 mm was evaluated for the whole patient group to understand the spectrum of variability and the percentage of cases that would have required a margin of approximately 1/5/10 mm if the diaphragm had been otherwise used for target localization.

Quantitative assessment of the lipiodol/diaphragm motion range on 4D-CBCT

The motion range in each direction obtained from the planning 4D-CT was compared with that of the treatment 4D-CBCT for the lipiodol and diaphragm. The motion difference between the 4D-CT and the 4D-CBCT with the lipiodol/diaphragm that was $\geq$3/5 mm was evaluated over all scans of each patient.

Statistical analysis

The patient mean (μ) and standard deviation (SD) of the interfractional changes of absolute lipiodol/diaphragm position were calculated over all 4D-CBCT scans, and from averaging the individual patient means, the group means (ΔM) were calculated. The pooled population systematic (Σ) and random errors (σ) were also calculated. Population statistics were also obtained for the tumor prediction error **e** for estimating the margin with the diaphragm-based correction protocol.

For statistical tests for correlations, one sample t-test for the difference of group mean from zero, and the two sample paired t-test for difference of motion range based on the diaphragm and lipiodol, MATLAB Statistical Toolbox (MathWorks Inc., Natick, MA, USA) was used. Statistical significance was considered with p-value <0.05.

Results

Quantitative assessment of the lipiodol/diaphragm position

Of 29 (55%) lipiodolized tumors, 16 showed contrast that qualified for the purpose of target localization on the 4D-CBCT and were entered in the subsequent analysis that included 87 4D-CBCT scans. The relationship between the absolute lipiodol and diaphragm centroid positions (Fig. 1) showed statistical significance in all directions, with Pearson's correlation coefficients (r) of 0.80 (LR), 0.78 (SI), and 0.83 (AP). The quantitative assessment of the lipiodol/diaphragm-based treatment setup and the tumor prediction error using lipiodol as the reference are listed in Tab. 1. The group means did not significantly differ between the absolute lipiodol and diaphragm positions for all directions, and insignificantly differ from 0 except for the CC direction where both lipiodol and diaphragm positioning showed an average offset of the estimated position towards the caudal direction with respect to the planning MidV position.

The absolute tumor prediction errors $|\bar{e}_{x/y/z}|$ were summarized for all selected fractions across all individuals and over each individual in Fig. 2. $|\bar{e}| \geq 5$ mm occurred in 12.5% of the patients in the CC direction, while $|\bar{e}| \geq 3$ mm was found in 19% of the patients in the LR, 31% in the CC, and 0% in the AP directions. For all fractions, maximum $|\bar{e}_{x/y/z}|$ were 7.6/11.1/6.4 mm. A larger lipiodol-to-diaphragm distance D in the planning 4D-CT scan was associated with a larger $|\bar{e}_{x/y}|$ ($p<0.05$) but not $|\bar{e}_z|$ ($p=0.23$; Fig. 3). Two patients who showed $|\bar{e}_y| > 5$ mm had $D > 6$ cm. Except for the AP direction in which the correlation between $|\bar{e}_z|$ and motion range was marginally significant ($p=0.058$), the tumor prediction errors $|\bar{e}_{x/y}|$ were statistically independent of the LR and CC motion ranges ($p>0.05$). The 4D registration results obtained with the lipiodol and diaphragm masks are shown in Fig. 4. When registration was made according to the diaphragm, noticeable target misalignment was observed, compared with the lipiodol reference.

Quantitative assessment of the lipiodol/diaphragm motion range

Variations of the motion range obtained from 4D registrations by the lipiodol and diaphragm averaged over all selected fractions are demonstrated for individual patients in Fig. 5. Mean variations in the motion range on the 4D-CBCT $\geq$5 mm relative to the reference 4D-CT for individuals were not infrequent, occurring for diaphragm-based registrations in 31% of the patients in the CC direction,

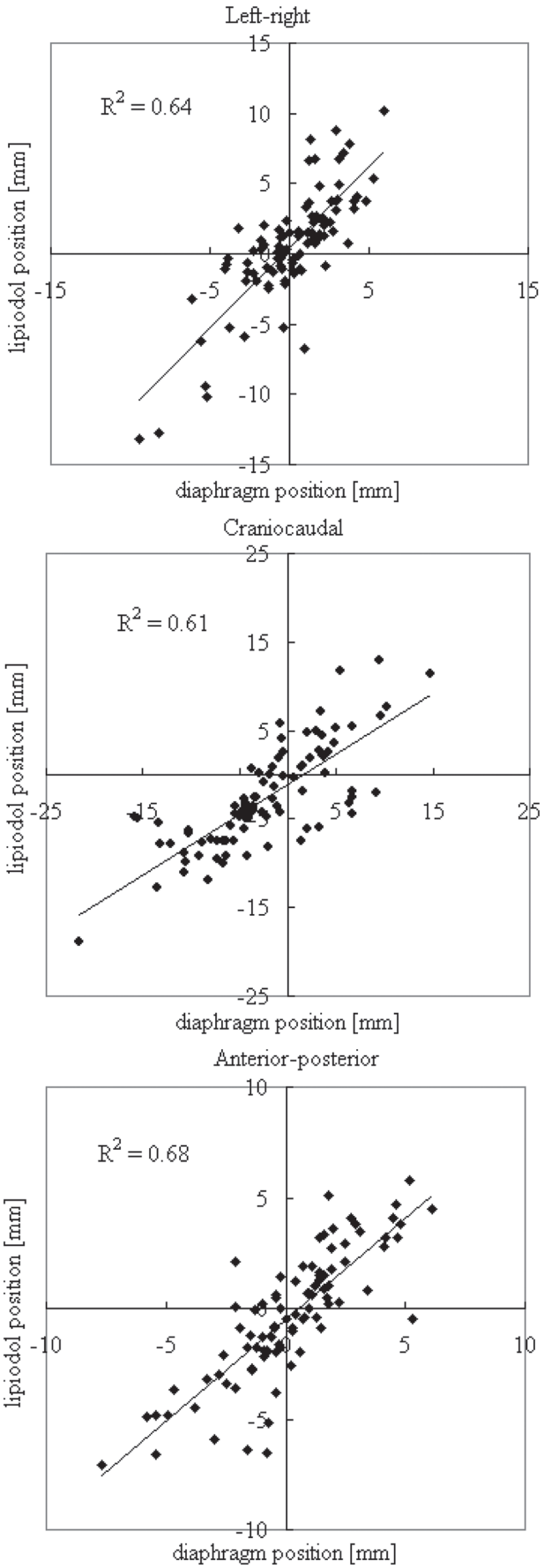

◀ **Fig. 1** Relationships of lipiodol and diaphragm positions for all fractions in the left–right, craniocaudal, and anteroposterior directions, respectively. The solid lines are the linear fits to the data points. Corresponding R^2 are also shown

Table 1 Population statistics of absolute lipiodol and diaphragm positions, and their differences between treatment setup 4D-CBCT and planning 4D-CT scans in terms of group means (*GM*), systematic errors (Σ), and random errors (σ)

	Left–right (mm)	Craniocaudal (mm)	Anteroposterior (mm)
Lipidol			
GM	0.5	−3.0	−0.5
Σ	3.5	4.7	1.8
σ	2.0	4.0	2.7
Diaphragm			
GM	0.0	−2.7	−0.1
Σ	2.1	5.6	1.2
σ	2.1	4.0	2.4
Lipiodol − diaphragm			
GM	0.4	−0.2	−0.7
Σ	2.1	3.8	1.0
σ	1.4	1.8	1.6

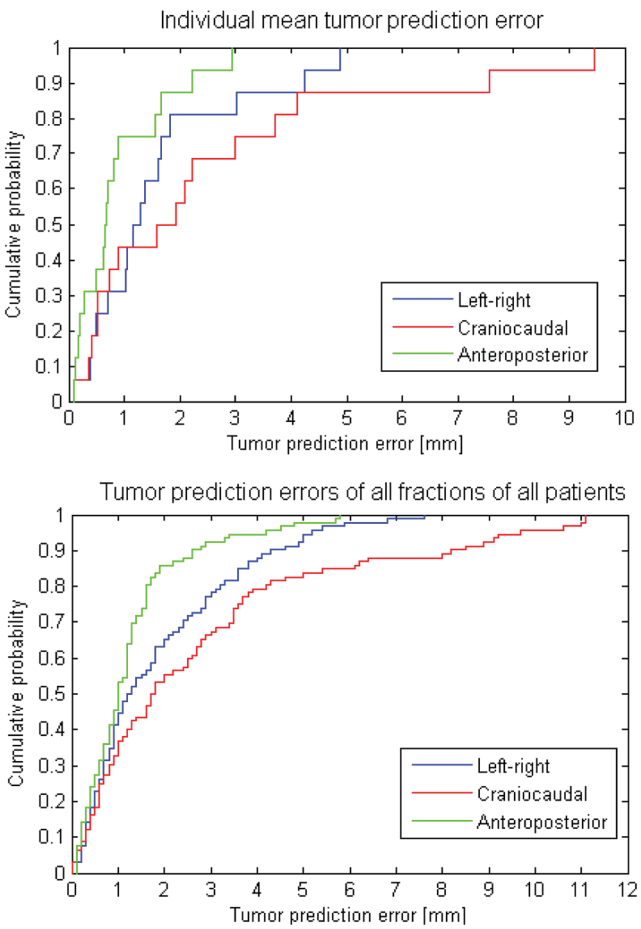

Fig. 2 Cumulative probability plots of the tumor prediction errors of individual means (*top*) and for all fractions of all patients (*bottom*)

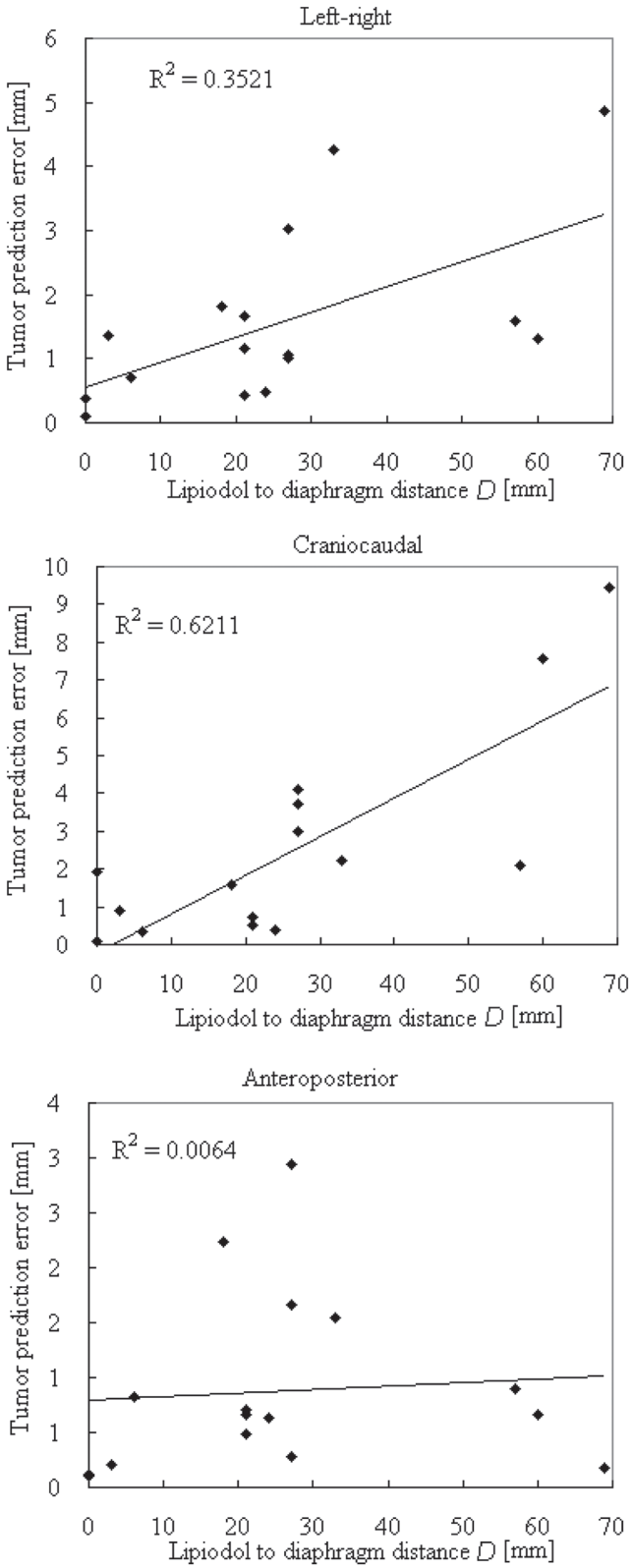

Fig. 3 Relationships between the lipiodol-to-diaphragm distance *D* and tumor prediction errors in three cardinal directions. Solid lines are the linear fits with corresponding R^2

while variations >3 mm were observed in 19 and 6% of the patients in the CC and AP directions for lipiodol-based registrations with 100% being increases of motion range, and 50 and 19% for diaphragm-based registration, of which 38 and 67% were increases. Mean absolute motion amplitude changes were 0.7, 1.8, and 0.8 mm for lipiodol and 1.1, 3.9, and 1.7 mm for the diaphragm in the LR, CC, and AP directions. Concerning those fractions that showed increases of motion range, the 95th percentiles were 2.4 (LR), 6.7 (CC), and 4.0 (AP) mm for lipiodol, and 2.4 (LR), 9.1 (CC), and 5.3 (AP) mm for the diaphragm. The LR and CC motion ranges estimated with the diaphragm were significantly larger ($p<0.05$) compared with the reference lipiodol.

Margin assessment

Combining the observed variations for lipiodol/diaphragm position, delineation, 4D registration and intrafractional baseline, into the van Herk's margin formula (see Methods and materials section), yields, without any image-guidance correction, the margins as shown in Fig. 6. When the variability of the diaphragmatic position was entered into the margin recipe, the resulting margins were either underestimated by 3.0 mm (LR) and 1.1 mm (AP), or overestimated by 2.1 mm (CC) with respect to those calculated with the lipiodol for the motion range from 0 to 20 mm.

The tumor prediction error alone contributed 5.6 (LR), 10.0 (CC), and 2.9 (AP) mm to the PTV margin even employing online 4D-CBCT due to the important systematic and random variations between the lipiodol and the diaphragm (Table 1). On top, 1.1 mm was enough to compensate for the (increasing) variations of motion range in all directions for all patients. Using our online lipiodol (diaphragm)-guided 4D-CBCT correction protocol yields margins as shown in Fig. 6. The possible gain in margin reduction from the online 4D-CBCT correction decreased from 5.3 (LR), 7.8 (CC), and 1.9 (AP) mm using the lipiodol-guided setup to 2.0 (LR), 2.0 (CC), and 0.7 (AP) mm with the diaphragm-guided setup with respect to those without any image-guided correction. In addition, the whole PTV should be shifted 3.0 mm in the caudal direction to correct for the group mean of the lipiodol and the diaphragm motion.

Discussion

Linac-integrated CBCT is a common IG tool for treatment verification in hypofractionated/stereotactic body radiotherapy of intrahepatic tumors. Nonetheless, the low soft-tissue contrast in CBCT makes visualization of the tumor almost impossible, and therefore anatomical or fiducial marker surrogates are often necessary to guide treatment verification.

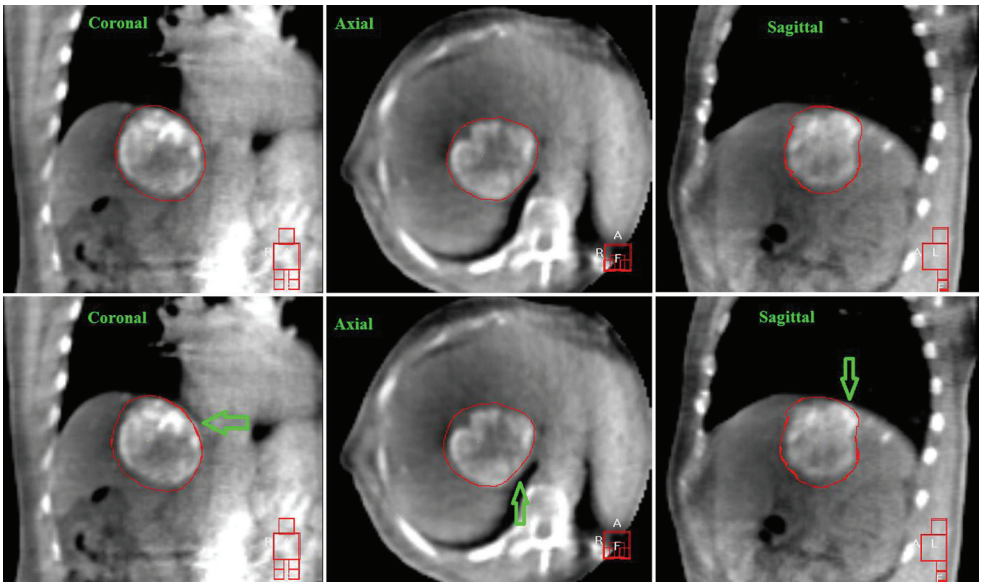

Fig. 4 Planning contour of the gross tumor volume (*GTV*) overlaid on the time-weighted average 4D-CBCT images after registration using lipiodol (*top row*) and the diaphragm (*bottom row*). Misalignment of the GTV was observed when target localization was made using the diaphragm as a surrogate, as indicated by the *arrows*

The effect of IV contrast was found to be seriously degraded on CBCT, and the signal-to-noise ratio of the IV contrast was very sensitive to the acquisition timing of CBCT [17]. Lipiodol during transarterial chemoembolization (TACE) was investigated as a direct surrogate for tumor localization previously [3, 18], but this study was the first to assess the potential of combining prior lipiodol contrast with on-line time-resolved 4D-CBCT. This treatment approach can not only take the therapeutic advantage of transarterial chemoembolization but also utilize lipiodol contrast as a direct tumor surrogate. Our preliminary clinical outcomes for primary HCC using this treatment method have demonstrating response rate of 67 % (with a median follow-up of 12 months), and 2-year overall survival rate of 54 %.

For patients without lipiodol contrast, diaphragm/liver contour is the most popular tumor surrogate. In a clinical evaluation, Guckenberger et al. [19] used free breathing 3D-CBCT for registration with the planning 4D-CT based on the liver contours at the exhale and inhale phases. Their benchmark results against the IV contrast-enhanced CT scans that were acquired with a mobile in-room CT found <3 mm difference in the LR and AP directions but up to 10 mm difference in the CC direction. The present work, which included the 4D information in the planning phase and treatment phase with 4D-CT simulation and 4D-CBCT verification, also found individual mean tumor prediction error up to 9.5 mm in the CC direction, suggesting that the differential motions between the diaphragm and tumor did play an important role.

For our cohort of 16 patients, the systematic tumor prediction error was found to be most important in the CC direction while the random contribution was roughly of the same order magnitude in the three directions and was comparable to those reported by Seppenwoolde et al. ([1]; 1.5–1.6 mm vs. 1.4–1.8 mm in this study). However, our observed systematic errors were slightly larger in the CC and LR directions than those of Seppenwoolde et al. [1]. As shown in Fig. 6, the significant systematic prediction error limits the potential of margin reduction, especially for the CC margin. If a diaphragm surrogate is used in the on-line correction protocol, a GTV-to-PTV margin of 5.6, 10.0, and 2.9 mm should be added in the LR, CC, and AP directions, respectively, to account for the offset of GTV's center of mass (COM) position from the liver contour's COM. On the other hand, the 3-mm shift in the caudal direction indicated by the group mean was likely due to the finite axial resolution (3 mm) of the 4D planning CT in comparison to the 4D-CBCT with 1 mm axial resolution. The shift may also come from the treatment room laser setup which at our institution was intended to offset by 0.5 mm from the radiation isocenter towards the cranial direction to align visually better with the mechanical crosshair at zero gantry degree for daily quality assurance purpose.

Even with dynamic IV-enhanced or lipiodol contrast, patient breath hold is still important for conventional 3D CBCT image acquisition to avoid significant motion artifacts caused by respiratory motion to obtain reasonable image quality. In a previous study of lipiodol-guided treatment setup, Yue et al. [3] acquired the 3D-CBCT by multiple breath holds. Although this strategy was useful to minimize respiratory motion, artifacts were still observed in their studies, possibly due to inconsistent anatomy between CBCT data acquisitions from different breath holds and/or residual motions such as heart beat and peristalsis. CBCT acquisitions in a single long breath hold have been demonstrated in one study showing a sharper outline of the diaphragm [20].

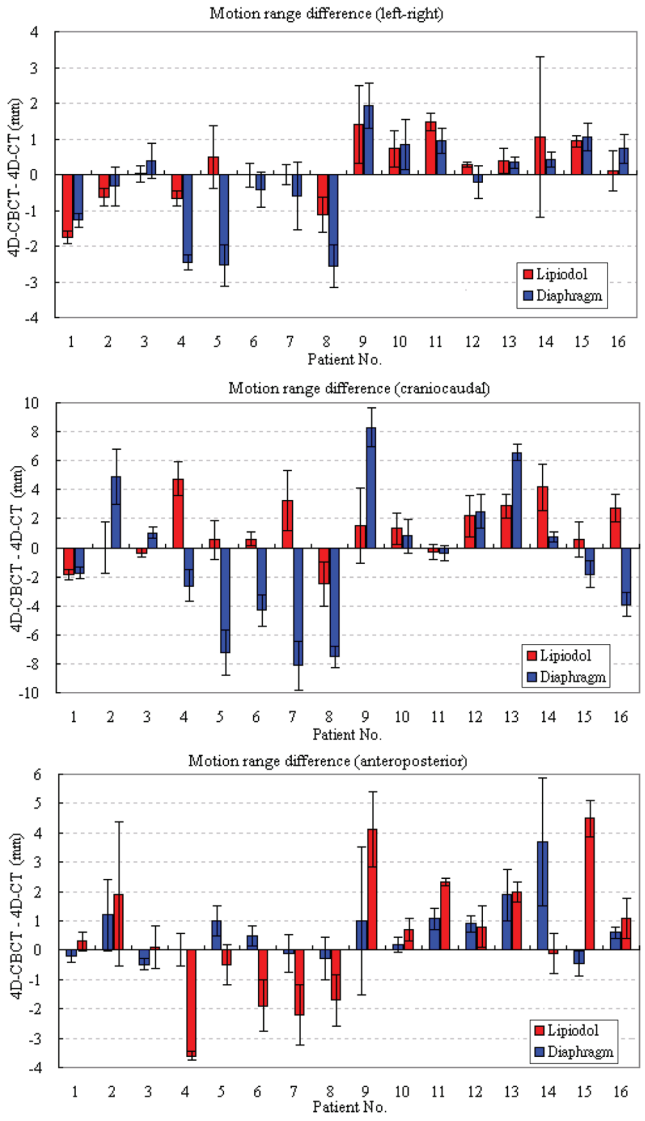

Fig. 5 Differences of the left–right, craniocaudal, and anterior–posterior motion ranges between 4D-CT and 4D-CBCT obtained by 4D registrations using the lipiodol and diaphragm masks

For our patients, it would have been extremely difficult for them to complete the CBCT scan in a single breath hold or even in multiple breath holds that usually had to last for >20 s. In our study, all patients underwent free breathing CBCT under optimized maximal abdominal compression. Such approach of planning and treating at the time-weighted average tumor position was not only suitable for all patients and also allowed a safety margin that is slightly larger than that for the breath hold approach because the systematic contribution due to tumor motion can be reduced to nearly zero, leaving a small random error (estimated using the SD of the tumor motion, or approximately one third of the tumor amplitude). Another advantage of 4D-CBCT over standard 3D-CBCT in free breathing treatment condition is the possibility of assessing the variation of motion range, which allowed us to halt the treatments if the increasing motion amplitude was well beyond the set tolerance (3 mm in our case). Variations of motion range with the lipiodol over all fractions for individuals were generally small, being less than 3 mm in the LR and 5 mm in the CC and AP directions for all patients. Similar results of 1.0 (LR), 1.7 (SI), and 1.6 (AP) mm were observed by Case et al. [9] although their estimates were based on the position of the diaphragm.

Our clinical implementation of diaphragm/lipiodol-guided 4D registration did not deal with anatomical deformations. A demonstration of finite element model (FEM)-based deformable image registration (DIR) for tumor positioning has been presented by Eccles et al. [21]. Their results found that the change of GTV's COM position was within 1 mm in all directions after rigid liver-to-liver registration for 16 patients under abdominal compression. The same group reported residual displacement of GTV's COM >3 mm in 15% of the treatment fractions for 12 patients imaged in breath hold [22], whereas our study found tumor prediction error >3 mm in 33% of the treatment fractions in the CC direction. The FEM-based DIR may be useful to predict the GTV's COM position where the GTV cannot be seen without IV/lipiodol contrast, but the poor efficiency because of the necessity of manual liver contouring on multiple CBCT datasets (for a 4D-CBCT scan) on top of the computational overhead thus far restricted its clinical implementation. Unlike the usual practice with fiducial markers or lipiodol deposit available for visual inspections, the DIR result of the deformed GTV's contour and COM cannot be directly confirmed, which may also concern the clinicians or radiotherapists. More importantly, using the deformed liver contour to infer via a biomechanical relationship the position of the interior GTV can have vector magnitude residual error as large as 4 mm, which necessitates a considerable PTV margin and, thus, hampering its potential as compared to lipiodol as a direct tumor surrogate.

In our study, almost all patients showed decreased lipiodol contrast on the 4D-CBCT as compared to on the 4D-CT, and about half of the lipiodolized tumors were abandoned for clinical setup because the lipiodol contrast was too low. The clinical implication of changing from lipiodol-guided to diaphragm-guided setup due to the absence of lipiodol contrast on 4D-CBCT without adapting the PTV margin may warrant further investigation. According to our initial experience, the visibility of the lipiodol deposit on the 4D-CBCT critically depended on its initial pattern on the planning CT, and that lipiodol deposits that showed higher Housfield Unit (HU) on the 4D-CT usually had better visualization on the 4D-CBCT than those with lower HU. For our clinical protocol, the lipiodol amount was limited to 20 ml to avoid liver failure. It was known that higher dose of lipiodol is needed for large and hypervascular HCC to attain complete filling of the tumor vessel bed. As reported

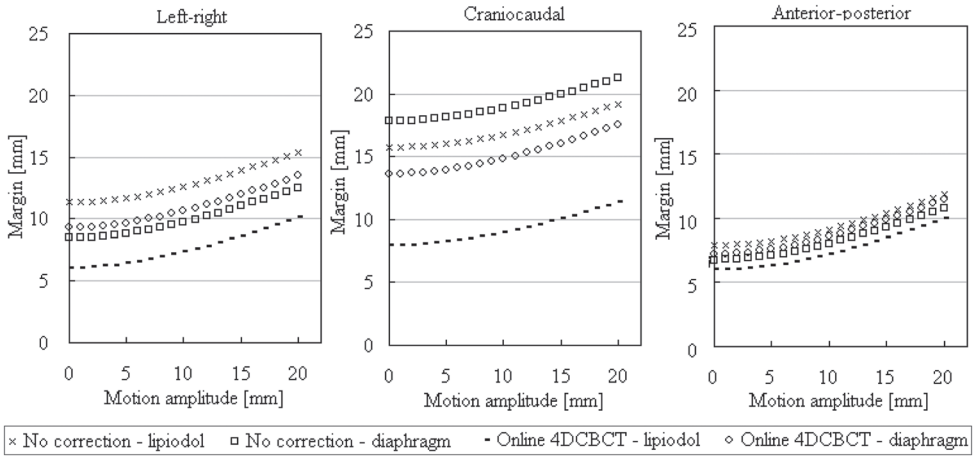

Fig. 6 Calculated left–right (*LR*), craniocaudal (*CC*), and anterior–posterior (*AP*) margins inclusive of delineation, 4D-CT to CBCT registration, and intrafractional baseline drift for different treatment approaches as a function of motion amplitude. For no image-guidance correction, the margins were calculated using the variations of lipiodol and the diaphragm, respectively. Margins for the online 4D-CBCT-lipiodol were obtained assuming ideal soft-tissue tumor correction protocol with zero systematic errors, while margins for the online 4DCBCT-diaphragm were obtained including the systematic and random errors due to the offset between the diaphragm and the lipiodolized tumor

in Chen et al. [16], lipiodol retention showing homogeneous and defective patterns was more frequent in the patient group receiving the high dose (20–53 ml) than that given the low dose (5–15 ml). Based on the initial findings of this study and previous reports, we have started to adjust the lipiodol volume to achieve better lipiodol contrast on 4D-CBCT for tumor localization.

Conclusion

Image guidance using lipiodol combined with 4D-CBCT enables accurate localization of HCC, thus, permitting significant reduction of uncertainty from the diaphragm surrogate and motion artifacts. A major limitation is the degraded lipiodol contrast on 4D-CBCT.

Compliance with ethical guidelines

Conflicts of interest M.K.H. Chan, V. Lee, CL. Chiang, F.A.S. Lee, G. Law, N.Y. Sin, K.L. Sui, F.C.S. Wong, S.Y. Tung, H. Luk, and O. Blanck state that there are no conflicts of interest. Part of the results of this work has been presented at the ESTRO 3rd forum.

The accompanying manuscript does not include studies on humans or animals.

References

1. Seppenwoolde Y, Wunderink W, Wunderink-van Veen SR, Storchi P, Méndez Romero A, Heijmen BJM (2011) Treatment precision of image-guided liver SBRT using implanted fiducial markers depends on marker-tumour distance. Phys Med Biol 56:5445–5468
2. Shin SW (2009) The current practice of transarterial chemoembolization for the treatment of hepatocellular carcinoma. Korean J Radiol 10:425–434
3. Yue J, Sun X, Cai J, Yin F-F, Yin Y, Zhu J, Lu J, Liu T, Yu J, Shi X, Song J (2012) Lipiodol: a potential direct surrogate for cone-beam computed tomography image guidance in radiotherapy of liver tumor. Int J Radiat Oncol Biol Phys 82:834–841. doi:10.1016/j.ijrobp.2010.12.050
4. Nakagawa K, Yamashita H, Igaki H, Terahara A, Shiraishi K, Yoda K (2008) Contrast medium-assisted stereotactic image-guided radiotherapy using kilovoltage cone-beam computed tomography. Radiat Med 26:570–572. doi:10.1007/s11604-008-0275-2
5. Sonke J-J, Zijp L, Remeijer P, van Herk M (2005) Respiratory correlated cone beam CT. Med Phys 32:1176–1186. doi:http://dx.doi.org/10.1118/1.1869074
6. Wolthaus J, Sonke J-J, Vanherk M, Belderbos J, Rossi M, Lebesque J, Damen E (2008) Comparison of different strategies to use four-dimensional computed tomography in treatment planning for lung cancer patients. Int J Radiat Oncol Biol Phys 70:1229–1238. doi:10.1016/j.ijrobp.2007.11.042
7. Sonke J-J, Rossi M, Wolthaus J, van Herk M, Damen E, Belderbos J (2009) Frameless stereotactic body radiotherapy for lung cancer using four-dimensional cone beam CT guidance. Int J Radiat Oncol Biol Phys 74:567–574. doi:10.1016/j.ijrobp.2008.08.004
8. Sonke J-J, Lebesque J, Vanherk M (2008) Variability of four-dimensional computed tomography patient models. Int J Radiat Oncol Biol Phys 70:590–598. doi:10.1016/j.ijrobp.2007.08.067
9. Case RB, Moseley DJ, Sonke JJ, Eccles CL, Dinniwell RE, Kim J, Bezjak A, Milosevic M, Brock KK, Dawson LA (2010) Interfraction and intrafraction changes in amplitude of breathing motion in stereotactic liver radiotherapy. Int J Radiat Oncol Biol Phys 77:918–925. doi:http://dx.doi.org/10.1016/j.ijrobp.2009.09.008
10. Case RB, Sonke J-J, Moseley DJ, Kim J, Brock KK, Dawson LA (2009) Inter- and intrafraction variability in liver position in non–breath-hold stereotactic body radiotherapy. Int J Radiat Oncol Biol Phys 75:302–308. doi:http://dx.doi.org/10.1016/j.ijrobp.2009.03.058
11. Srimathveeravalli G, Leger J, Ezell P, Maybody M, Gutta N, Solomon SB (2013) A study of porcine liver motion during respiration for improving targeting in image-guided needle placements. Int J Comput Assist Radiol Surg 8:15–27. doi:10.1007/s11548-012-0745-y

12. Yang J, Cai J, Wang H, Chang Z, Czito BG, Bashir MR, Palta M, Yin F-F (2014) Is diaphragm motion a good surrogate for liver tumor motion? Int J Radiat Oncol Biol Phys 90:952–958. doi:http://dx.doi.org/10.1016/j.ijrobp.2014.07.028
13. Chan MKH, Kwong DLW, Law GML, Tam E, Tong A, Lee V, Ng SCY (2013) Dosimetric evaluation of four-dimensional dose distributions of CyberKnife and volumetric-modulated arc radiotherapy in stereotactic body lung radiotherapy. J Appl Clin Med Phys 14:4229
14. Velec M, Moseley JL, Brock KK (2014) Simplified strategies to determine the mean respiratory position for liver radiation therapy planning. Pract Radiat Oncol 4:160–166
15. van Herk M, Remeijer P, Rasch C, Lebesque J (2000) The probability of correct target dosage: dose-population histograms for deriving treatment margins in radiotherapy. Int J Radiat Oncol Biol Phys 47:1121–1135
16. Chen M, Li J, Zhang Y, Lu L, Zhang W, Yuan Y, Guo Y, Lin X, Li G (2002) High-dose iodized oil transcatheter arterial chemoembolization for patients with large hepatocellular carcinoma. World J Gastroenterol 8:74–78
17. Jones BL, Altunbas C, Kavanagh B, Schefter T, Miften M (2014) Optimized dynamic contrast-enhanced cone-beam CT for target visualization during liver SBRT. J Phys Conf Ser 489:012035
18. Hawkins MA, Brock KK, Eccles C, Moseley D, Jaffray D, Dawson LA (2006) Assessment of residual error in liver position using kV cone-beam computed tomography for liver cancer high-precision radiation therapy. Int J Radiat Oncol Biol Phys 66:610–619. doi:http://dx.doi.org/10.1016/j.ijrobp.2006.03.026
19. Guckenberger M, Sweeney RA, Wilbert J, Krieger T, Richter A, Baier K, Mueller G, Sauer O, Flentje M (2008) Image-guided radiotherapy for liver cancer using respiratory-correlated computed tomography and cone-beam computed tomography. Int J Radiat Oncol Biol Phys 71:297–304. doi:10.1016/j.ijrobp.2008.01.005
20. Zhong R, Wang J, Jiang X, He Y, Zhang H, Chen N, Bai S, Xu F (2012) Hypofraction radiotherapy of liver tumor using cone beam computed tomography guidance combined with active breath control by long breath-holding. Radiother Oncol. doi:10.1016/j.radonc.2011.11.007
21. Eccles CL, Dawson LA, Moseley JL, Brock KK (2011) Interfraction liver shape variability and impact on GTV position during liver stereotactic radiotherapy using abdominal compression. Int J Radiat Oncol Biol Phys 80:938–946. doi:http://dx.doi.org/10.1016/j.ijrobp.2010.08.003
22. Brock KK, Hawkins M, Eccles C, Moseley JL, Moseley DJ, Jaffray DA, Dawson LA (2008) Improving image-guided target localization through deformable registration. Acta Oncol 47:1279–1285. doi:10.1080/02841860802256491